The Optical Properties of the Woodburytype - An Alternative Printing Technique Based on a Gelatine/Pigment Matrix

D. J. Leech, W. Guy, S. Klein

Centre for Fine Print Research, University of the West of England, Bristol BS3 2JT, United Kingdom

E-mail: damien.leech@uwe.ac.uk, susanne.klein@uwe.ac.uk

Abstract. The Woodburytype is a 19th century photomechanical technique, producing high-quality continuous-tone prints that use a mixture of pigment and gelatine as a relief print, in which the variation in height of the print produces the tone and contrast. We propose a simple optical model for the process based on Kubelka-Munk theory that takes into account the ink formulation, the print height and the substrate surface in order to provide the ideal combination of printing depth and contrast.

1. Introduction

Printing methods have traditionally been utilised to mass produce items - at a low cost and with a large throughput. Both modern and more traditional processes, including screen, gravure and inkjet printing, have all been exploited across a broad number of scientific fields, such as for the production of flexible electronics [1], biosensors [2] and optical lenses [3]. Therefore, knowledge of these processes and their alternatives can be useful in determining not only the optimal printing method to attain the highest yield and throughput, but also for the identification of other possible applications.

The Woodburytype printing process was invented by Walter B. Woodbury and patented in 1863 [4]. It was the first, and still remains the only, photomechanical process that can reproduce truly continuous tone since the image is not broken up in dots or pixels but generated by a relief of pigmented gelatine layers.

A Woodburytype print is pulled from a relief printing plate which is filled with a pigmented gelatine ink. After the ink has dried, the tone of the print is achieved by variations of the print height and therefore of the probability that photons are absorbed or scattered as they pass through the print. The higher the attenuation coefficient and the longer the light path through the medium, the darker the tone. We suggest a simple optical model to predict the optimal carbon black pigment concentration for a given printing plate depth in order to achieve the largest possible contrast and grayscale.

2. Experimental Methods - Ink Formulation & Optical Measurements

2.1. Ink Formulation

The gelatine inks for Woodburytype used here consist of 17.5wt% of gelatine, 82.5wt% of de-ionised water and 0.005 to 0.1 wt% of carbon black. The gelatin used was Rousselot 250 bloom food grade gelatine (Rousselot, used as received) and the carbon black was XPB 430 (Orion engineered carbon, used as received), an easy to disperse carbon black pigment preparation with 50wt% pigment. Half of the DI water was added to the gelatine and the mixture was left to swell. The pigment was dispersed in the rest of the water and added to the water gelatine mixture, when all the water was absorbed by the gelatine. The final mixture was melted in a low temperature oven at 50°C. To age the gelatine, the ink was put into a fridge at 6°C for 12 hours and then heated up to 40°C for printing.

2.2. Printing process

In order to obtain quantitative data, we use a step-wedge silicon printing plate that consists of eleven equally spaced and adjacent steps with depths between 0 mm and 1 mm, as seen in Fig. 1. These steps are 1 cm $\times$ 1 cm in width, to ensure they are larger than the viewing aperture of our optical measurement equipment. The printing process involves filling the plate with a surplus of the gelatine ink, placing paper onto

Figure 1. Left: Example of the Woodburytype printing process, mounted on card. The ink used has a pigment content of 0.015%. Right: Print next to the step-wedge printing plate, after being pulled. The ink used here has a pigment content of 0.025%.

the filled plate and transferring the ink to the paper by exposing it to pressure in a letter press until the ink has set. The compression time, between 5 to 10 minutes, depends on the amount of gelatine contained in the ink - a larger weight percentage will lead to a shorter setting time. As a release agent, lavender oil was applied to the plate prior to printing to ensure that the ink transfers to the paper surface. We use glossy photographic microporous ink-jet paper (SKU PPD-68) in order to minimze ink absorption by the paper. Each print is repeated three times to ensure we obtain at least one print free from visually-obvious defects, such as air bubbles or edge tears.

2.3. CIELAB Measurements

To determine the contrast and grayscale, we used a Konica-Minolta FD-7 spectrometer to represent the data in the CIELAB coordinate system [5]. It is defined by three variables, L^*, a^* and b^*. L^* represents the 'lightness', ranging from 0 (dark) to 100 (light), a^* the green-red and b^* the yellow-blue colour components, that range from -100 to 100, respectively. These are mathematically accessed via the CIEXYZ colour space, comprised of the three tristimulus values X, Y and Z, that are similar but less perceptively uniform.

As we are currently concerned with monochromatic prints, we use only the value of L^*, which is linked to the Y tristimulus value via

$$L^* = 116f\left(\frac{Y}{Y_n}\right) - 16, \tag{1}$$

where $Y_n = 100$, the value for the normalized white point of a colour temperature of 6500 K, $\delta = 6/29$ and $f(t) = t^{1/3}$ if $t > \delta^3$ or $f(t) = t/3\delta^3 + 4/29$ if $t < \delta^3$. The tristimulus value Y itself has the form

$$Y = 100\sum_{\lambda}\frac{R(\lambda)S(\lambda)\bar{y}(\lambda)\Delta\lambda}{S(\lambda)\bar{y}(\lambda)\Delta\lambda}, \tag{2}$$

where $S(\lambda)$ is the relative spectral power distribution, $R(\lambda)$ is the spectral reflectance factor and $\bar{y}(\lambda)$ is one of the three colour matching functions used in the CIEXYZ colour space. We use a standardized D65 illuminant, comparable to the black body radiation of an object at $T = 6500$ K, and so $\bar{y}(\lambda)$ has a form given by the approximation in Ref. [6].

3. Optical Model

3.1. Kubelka-Munk Theory

Kubelka-Munk theory is a radiative transfer model that characterises the properties of optically turbid media such as paint or ink films. It models a layer as a continuous medium, rather than a ensemble of individual pigment particles, in order to ignore complex multiple-scattering effects and characterises the film with an absorption K and scattering coefficient S, per unit length [7]. It is assumed that these coefficients are uniform throughout the thickness of the film and that there are no prominent boundary effects, such that the plane has an effectively infinite width and length.

Multiple attempts have been made to link these Kubelka-Munk (KM) coefficients, K and S, with the properties of the individual pigment particles [8, 9, 10, 11, 12], however the exact relationship seems to vary greatly depending on the ratio between K and S. As such, Kubelka-Munk theory is seen as a purely phenomenological approach and is also therefore pigment dependent.

The reflectance $R(\lambda)$ of a film on a substrate can therefore be predicted via the KM coefficients as [9]

$$R = \frac{1 - R_g\left(a - b\coth bSd\right)}{a - R_g + b\coth bSd}, \tag{3}$$

where

$$a = \frac{S+K}{S}, \quad b = \sqrt{a^2 - 1}. \tag{4}$$

These equations dictate how the reflectance changes with the substrate reflectance R_g (that ranges between 0 and 1 for a transparent and specular reflector, respectively)

and film thickness, d. The reflectance of carbon black varies minimally in the visible region [13] and so we assume it is effectively constant across these wavelengths. The reflectance tends toward a set value R_∞, that describes a layer providing zero transmission, that can instead be calculated by

$$R_\infty = 1 + \frac{K}{S} - \sqrt{\left(\frac{K}{S}\right)^2 + 2\left(\frac{K}{S}\right)}. \tag{5}$$

It is through these reflectance values that we can link the CIELAB values to the KM coefficients and therefore parameterize the inks we are using.

The print height d of the Woodburytype print is of huge importance, as it varies to a greater degree than in a traditional print. A known gelatine content in the ink formulation means that we can estimate the print height, purely from the trough depths of our printing plate. Using the fact that the steps have dimensions $1 \times 1 \times Z$ mm, where Z varies between 0.1 and 1 mm, the ratio between the volume of the gelatine and the total mixture should give us an estimate of the print height once dry. We neglect the presence of carbon as this represents, at most, 1% of the dry mixture. The ratio in this recipe is given by densities of $\rho_{gel} = 1.3$ g/cm^3 [14] so that the volume of gelatine in the recipe is $V_{gel} = 15/1.3 = 11.5385$ cm^3 and the ratio is $V_{gel}/V_{tot} = 0.1415$. Therefore in the deepest step with height 1 mm, the print height should be $d = 0.1415 \times 1 = 0.1415$ mm $= 142$ μ m. We assume that these heights are directly proportional to the step depth and scale based on this value. The optical path length is double the print height. Gelatine heights measured by Scanning Electron Microscopy (SEM), shown in blue in Fig. 2, show a similar trend to the above calculation.

Fig. 3 shows the CIELAB results for thirteen differing inks in red. The pigment concentrations increase in rough steps of 0.005% carbon content below 0.02% and in steps of 0.02% above that to closely map the sharp decay of the data at those lower pigment concentrations. The photographic paper used has a CIELAB brightness of $L^* = 93.3$ and provides an upper limit to the data set. As expected, the general trend is an exponential decay toward a minimum value of $L^* = 6.5$ with increasing pigment concentration, corresponding to the presence of a minimum reflectance value, R_∞.

3.2. Single Coefficient Fitting

Using the equations previously defined for reflectance, we can use various values of the KM coefficients, K and S, in order to predict the L^* curve for a particular concentration. If we assume that all particles dispersed in the gelatine matrix can be considered identical, we can define the absorption and scattering coefficients within the Kubelka-Munk theory in terms of the absorption and scattering cross sections

$$K = f\frac{C_{Abs}}{V}, \qquad S = f\frac{C_{Sca}}{V}, \tag{6}$$

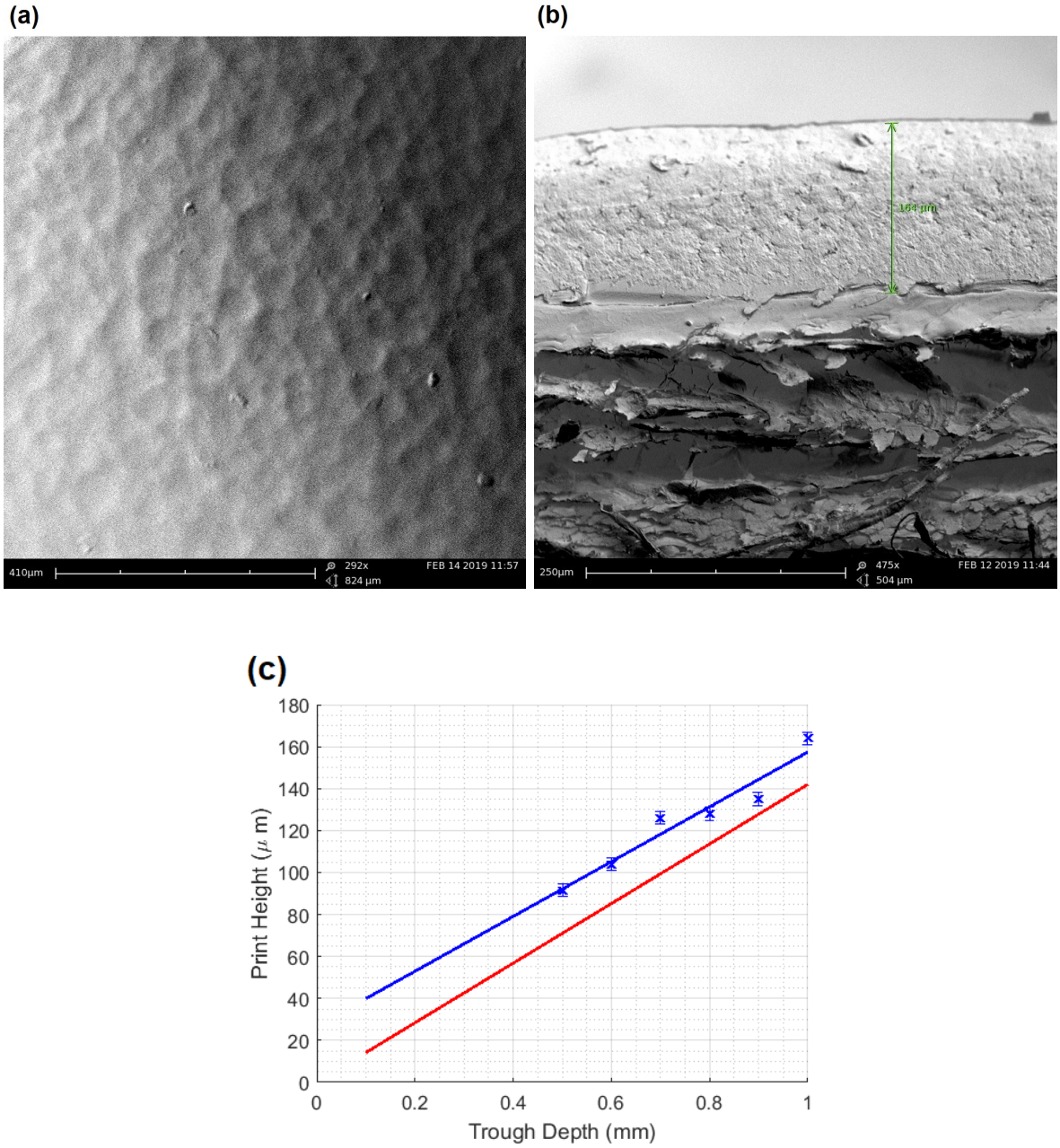

Figure 2. (a) Scanning electron micrograph of the paper surface - as the surface is distinctly cratered, we can assume it will therefore provide a diffuse reflectance. (b) Example of the measurement of the gelatine print height, via imaging of the print 'edge-on'. Below the print is the paper, now split during the process of drying due to the constriction of the gelatine. (c) Dried print height against the depth of the trough on the printing plate. We take a general trend, in blue, in order to minimise the variations in the print height. The red line represents the simple estimation based on the proportion of gelatine in the ink, as described in the text.

where V is the volume of one such particle and f is the particle volume fraction [13],

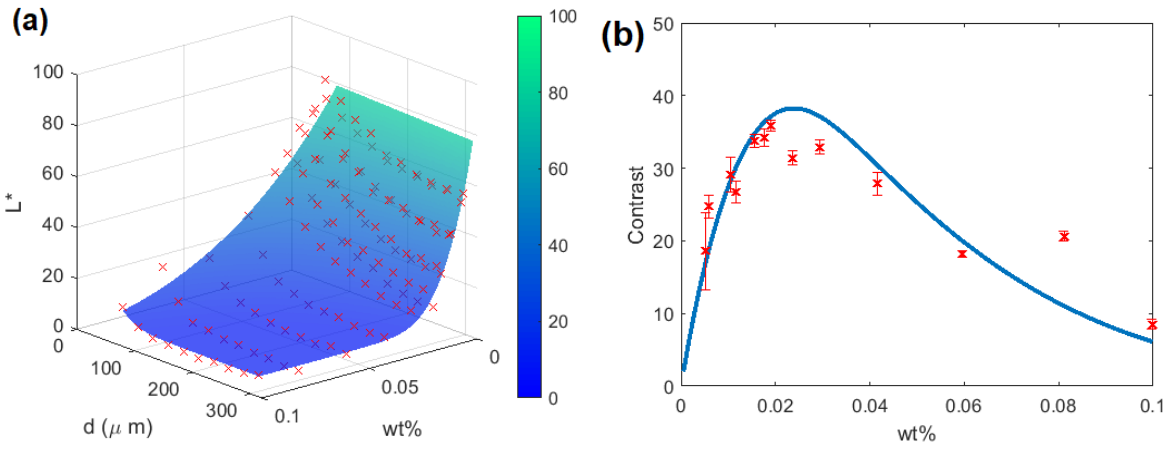

Figure 3. (a) CIELAB results of the step wedge prints for varying weight percentages, the data points are seen in red. A higher concentration of pigment results in a darker print, as expected, and the prints in general tend toward a minimum non-zero L^* value. Note that additional fitting has been implemented, using the value of the paper reflection R_g. (b) The contrast of a step wedge print, calculated as the max difference in L^*, for inks of varying weight percentage and comparing the results (red crosses) and theory (blue line).

that can be related to the particle weight fraction F via

$$f = \left[1 + \frac{\rho_{car}}{\rho_{gel}}\left(\frac{1-F}{F}\right)\right]^{-1}, \tag{7}$$

where $\rho_{car} = 1.8$ g/cm^3 [15] and $\rho_{gel} = 1.3$ g/cm^3 [14] and a particle weight fraction between 0.1% and 1.1%.

We then use these scaled KM coefficients to predict the L^* curve and use the mean squared error method to characterize the deviation from the data set. With n data points y, alongside the same number of calculated points $\bar{y}$, the mean squared error of such a data set is

$$MSE = \frac{1}{n}\sum_{1}^{n}(y-\bar{y})^2\,. \tag{8}$$

We minimise this value by varying the variable set $\{C_{Abs}/V, C_{Sca}/V, R_g\}$ to provide the best fit for the data set. We find this minima exists for $C_{Abs}/V = 3.20 \times 10^6$, $C_{Sca}/V = 0.06 \times 10^6$ and $R_g = 0.57$ and is similar in magnitude to the results found in Ref. [13], with a slight underestimation of the absorption term. The results of this fitting can be seen in Fig. 3, against the original data set.

We can then extend this by plotting the full L^* dependence and discerning the contrast of each possible print as the difference between the L^* values of the largest and smallest trough of our step-wedge. Fig. 3b displays the results of such a dependence, comparing both the measured results and the theoretical expectation values, and shows the distinct region of inks that should provide the largest contrast congregates around a weight percentage of 0.02%. The CIELAB results, averaged across three measurements, for three inks, including one around the high contrast maxima, can be seen in Table 1.

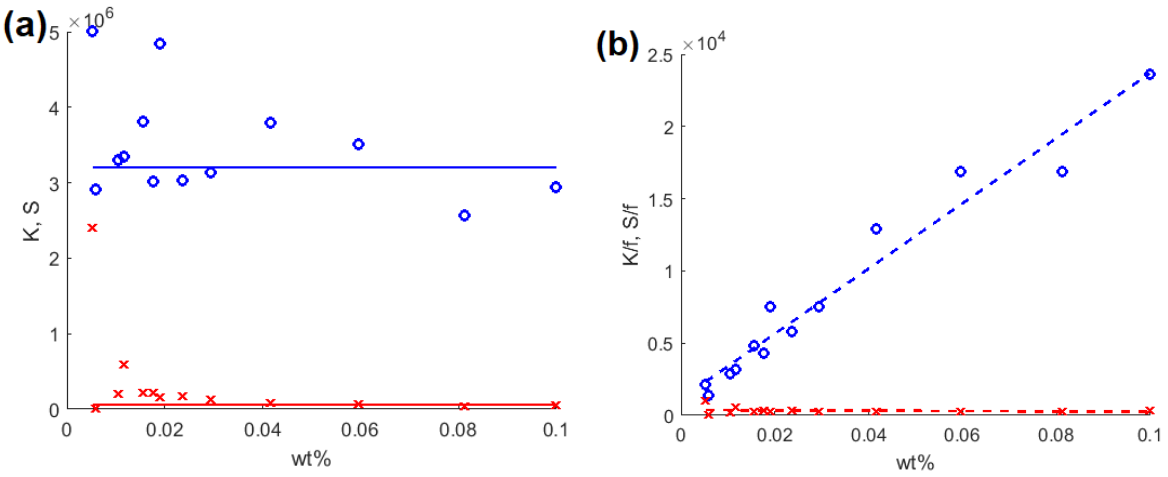

Figure 4. (a) KM coefficients fitted per weight percentage and therefore per print. Blue points represents the absorption term K and red the scattering term S. The solid lines represent the values found previously in Fig. 3. (b) The variation in value in the KM coefficients per print, scaled by the volume fraction. A dashed line of best fit is added to highlight that the absorption term scales linearly with volume fraction and the scattering remains relatively constant and small, with a small increase for extremely weak pigment inks.

3.3. Multiple Coefficient Fittings

As a first approximation, we have ignored any of optical properties of the binding gelatine that comprises the majority of the print, justified by the hugely absorbant nature of the pigment used. However it is feasible to assume that as the weight percentage decreases, the optical effects of the gelatine should emerge more prominently and the absorption and scattering coefficients could change.

We test this assumption by allowing the characteristic absorption and scattering, K and S, to change between inks and therefore with the weight percentage. The value of the reflectance of the substrate R_g is assumed to be constant during this variation and takes the value of the previous fitting. The results of this process can be seen in Fig. 4a - each print and therefore ink formulation is now described by a unique set of KM coefficients. A comparison to the single coefficient fitting is represented by the solid lines. When scaled by the volume fraction, as in Fig. 4b, the overall relationship is more obvious, with a positive gradient for the absorption term and a mild negative

Table 1. CIELAB Results of 3 Woodburytype inks; the lightest, the largest contrast and the darkest.

wt%	0.1	0.2	0.3	0.4	0.5	0.6	0.7	0.8	0.9	1.0
0.0052	75.12	70.12	66.27	63.18	59.77	58.93	57.93	56.53	56.83	58.02
0.0190	53.12	41.78	33.89	29.29	25.20	23.11	19.05	17.27	16.25	16.45
0.0998	15.31	9.72	7.42	7.00	6.62	6.48	7.00	6.78	7.12	8.52

gradient for the scattering term.

Overall, the values remain somewhat consistent above weight percentages 0.02%, but scattering is enhanced below this value. This could be the result of the increase of the contribution of the optical properties of the background gelatine with decreasing pigment concentration. It results in a lower limit to our model that could explain the underestimation of the absorption given by the single coefficient fitting.

4. Conclusion

Single and multiple coefficient fitting lead to similar results for the absorption and scattering terms and therefore a pigment load of about 0.02wt% for maximum contrast for a printing plate with a maximum depth of 1 mm. The region of maxima in Fig. 3 is somewhat flat and therefore provides a range of values with large contrast, that can be pushed toward lighter prints (higher values of L^*) for lower weight percentages and darker prints for higher weight percentages. Optimising the pigment load for a given relief depth will lead to maximal contrast and grayscale. However, larger contrast could theoretically be attained, aside from the ink formulation, by including relief depths larger than that maximum threshold currently used, although due to the exponential decay of the L^* values this will have increasingly diminishing returns. L^* values will also be dependent on the surface topography and the colour of the substrate which, while not considered here, will be integral in determining a generic relationship between the Woodburytype ink, the depth of the printing plate and the optical appearance of the print.

References

[1] D. Li, Y. Z. Zhang and W. Huang, Printable Transparent Conductive Films for Flexible Electronics, *Adv. Mat.* **30,** 1704738 (2018).

[2] J. Li, F. Rossignol and J. MacDonald, Inkjet printing for biosensor fabrication: combining chemistry and technology for advanced manufacturing, *Lab on a Chip* **15,** 2538 - 2558 (2015).

[3] J. Alamán, R. Alicante, J. I. Peña and C. Sánchez-Somolinos, Inkjet Printing of Functional Materials for Optical and Photonic Applications, *Materials* **9,** 910 (2016).

[4] W. Crawford, The Keepers of Light, Morgan & Morgan, Dobbs Ferry, New York (1979).

[5] J. Schanda, Colorimetry: Understanding the CIE System, CIE Central Bureau, Vienna (2006).

[6] C. Wyman, P. P. Sloan and P. Shirley, Simple Analytic Approximations to the CIE XYZ Color Matching Functions, *Journal of Computer Graphics Techniques* **2,** 2 (2013).

[7] P Kubelka and F. Munk, Ein Beitrag zur Optik der Farbanstriche, Zeitschrift fr Technische Physik **12,** 593 - 601 (1931).

[8] P. S. Mudgett and L. W. Richards, Multiple Scattering Calculations for Technology, *Applied Optics* **10,** 1485 - 1502 (1971).

[9] M. Quinten, The color of finely dispersed nanoparticles, *Applied Physics B* **73,** 317 - 326 (2001).

[10] L. Yang and B. Kruse, Revised Kubelka-Munk theory. I. Theory and application, *Journal of the Optical Society of America A* **21,** 1933 - 1941 (2004).

[11] H. Granberg and P. Edström, Quantification of the Intrinsic Error of the Kubelka-Munk Model Caused by Strong Light Absorption, *Journal of Pulp and Paper Science* **29,** 386 - 390 (2003).

[12] L. E. McNeil and R. H. French, Light scattering from red pigment particles: Multiple scattering in a strongly absorbing system, *Journal of Applied Physics* **89,** 1 (2000).

[13] T. Tesfamichael, A. Hoel, G. A. Niklasson, E. Wckelgrd, M. K. Gunde and Z. C. Orel, Optical characterization method for black pigments applied to solar-selective absorbing paints, *Applied Optics* **40,** 1672 - 1681 (2001).

[14] N. G. Parker and M. J. W. Povey, Ultrasonic study of the gelation of gelatin: Phase diagram, hysteresis and kinetics, *Food Hydrocolloids* **26,** 99-107 (2012).

[15] What is Carbon Black? https://www.thecarycompany.com/media/pdf/specs/orion-what-is-carbon-black.pdf Accessed 04/03/2019.